AMSR-E/Aqua L2A Global Swath Spatially-Resampled Brightness Temperatures, Version 3

USER GUIDE

How to Cite These Data

As a condition of using these data, you must include a citation:

Ashcroft, P. and F. J. Wentz. 2013. *AMSR-E/Aqua L2A Global Swath Spatially-Resampled Brightness Temperatures, Version 3*. [Indicate subset used]. Boulder, Colorado USA. NASA National Snow and Ice Data Center Distributed Active Archive Center. https://doi.org/10.5067/AMSR-E/AE_L2A.003. [Date Accessed].

FOR QUESTIONS ABOUT THESE DATA, CONTACT NSIDC@NSIDC.ORG

FOR CURRENT INFORMATION, VISIT https://nsidc.org/data/AE_L2A

National Snow and Ice Data Center

TABLE OF CONTENTS

1 DATA DESCRIPTION

1.1 File Information

1.1.1 Format

Level-2A brightness temperature files contain three swaths in HDF-EOS format:

1.1.1.1 Low_Res_Swath:

All channel observations, except for 89.0 GHz, at a nominal interval of 10 km; 243 observations per approximately 2000 scans.

1.1.1.2 High_Res_A_Swath:

89 GHz observations from the A feedhorn AMSR-E scans; 486 observations per approximately 2000 scans. Note: Beginning 4 November 2004, the 89 GHz A-horn developed a permanent problem resulting in a loss of those observations. Consequently, after 3 November 2004, the High_Res_A_Swath data fields contain values of 0.

1.1.1.3 High_Res_B_Swath:

89 GHz observations from the B feedhorn AMSR-E scans; 486 observations per approximately 2000 scans.

1.1.2 Data Fields

Each file contains the following contents. See the appendices of this document for a list of all HDF-EOS fields. Data also contain core metadata and product-specific attributes.

- Low Res Swath Data Fields
- High Res A Swath and High Res B Swath Data Fields
- Geolocation Fields
- Global Attributes

Level-2A files contain data elements transferred directly from Level-1A antenna temperatures, but without 1:1 mapping. Users should match the two sets of data by the corresponding time of acquisition. Missing brightness temperature data are indicated by 0. Antenna temperature coefficients, effective hot load temperatures, calibration counts, and antenna coefficients are only provided for users who want to see how brightness temperatures were calculated for this data set. They are not required to view brightness temperatures.

Antenna temperature coefficients are three-dimensional arrays (3,10,2001). The first component represents slope, offset, and a quadratic term. The quadratic term is zero for all channels except 6.9 GHz. Brightness Temperatures (T_b) are not calculated for the first and last scans. All other scans have two non-zero coefficients for all channels, except 6.9 GHz, which has three non-zero coefficients. The last component is the number of scans per granule; it is variable.

For data with scale and offset values, the data values can be obtained in the specified units with the following equation:

data value in units = (stored data value * scale factor) + offset

Example: T_b (kelvin) = (stored data value * 0.01) + 327.68

Scaling factors and offsets are provided with the local attributes of each HDF-EOS file. You should check each file to ensure correct values.

For more information on the L1 data fields' format descriptions transferred to L2A, see Aqua AMSR-E Level 1 Product Format Description Document

1.1.3 File Contents

Each half-orbit granule is approximately 58 MB using HDF compression.

The daily data rate is approximately 2.5 GB. Each half-orbit granule is approximately 58 MB using HDF compression.

1.1.4 Naming Convention

This section explains the file naming convention used for this product with an example. The date and time correspond to the first scan of the granule.

Example file names:

- `AMSR_E_L2A_BrightnessTemperatures_B01_200206012358_A.hdf`
- `AMSR_E_L2A_BrightnessTemperatures_X##_yyyymmddhhmm_f.hdf`

Refer to Table 1 for the valid values for the file name variables.

Table 1. Valid Values for the File Name Variables

Variable	Description
X	Product Maturity Code

Variable	Description
##	file version number
yyyy	four-digit year
mm	two-digit month
dd	two-digit day
hh	hour, listed in UTC time, of first scan in the file
mm	minute, listed in UTC time, of first scan in the file
f	orbit direction flag (A = ascending, D = descending)
hdf	HDF-EOS data format

Table 2. Valid Values for the Product Maturity Code

Product Maturity Code	Description
P	Preliminary - refers to non-standard, near-real-time data available from NSIDC. These data are only available for a limited time until the corresponding standard product is ingested at NSIDC.
B	Beta - indicates a developing algorithm with updates anticipated.
T	Transitional - period between beta and validated where the product is past the beta stage, but not quite ready for validation. This is where the algorithm matures and stabilizes.
V	Validated - products are upgraded to Validated once the algorithm is verified by the algorithm team and validated by the validation teams. Validated products have an associated validation stage.

Table 3. Validation Stages

Validation Stage	Description
Stage 1	Product accuracy is estimated using a small number of independent measurements obtained from selected locations, time periods, and ground-truth/field program efforts.
Stage 2	Product accuracy is assessed over a widely distributed set of locations and time periods via several ground-truth and validation efforts.
Stage 3	Product accuracy is assessed, and the uncertainties in the product are well-established via independent measurements made in a systematic and statistically robust way that represents global conditions.

Table 4. Related File Extensions and Descriptions

Extensions for Related Files	Description
.jpg	Browse data
.qa	Quality assurance information
.ph	Product history data
.xml	Metadata files

1.2 Spatial Information

1.2.1 Coverage

Coverage is global between 89.24°N and 89.24°S. See AMSR-E Pole Hole for a description of holes that occur at the North and South Poles. The swath width is 1445 km.

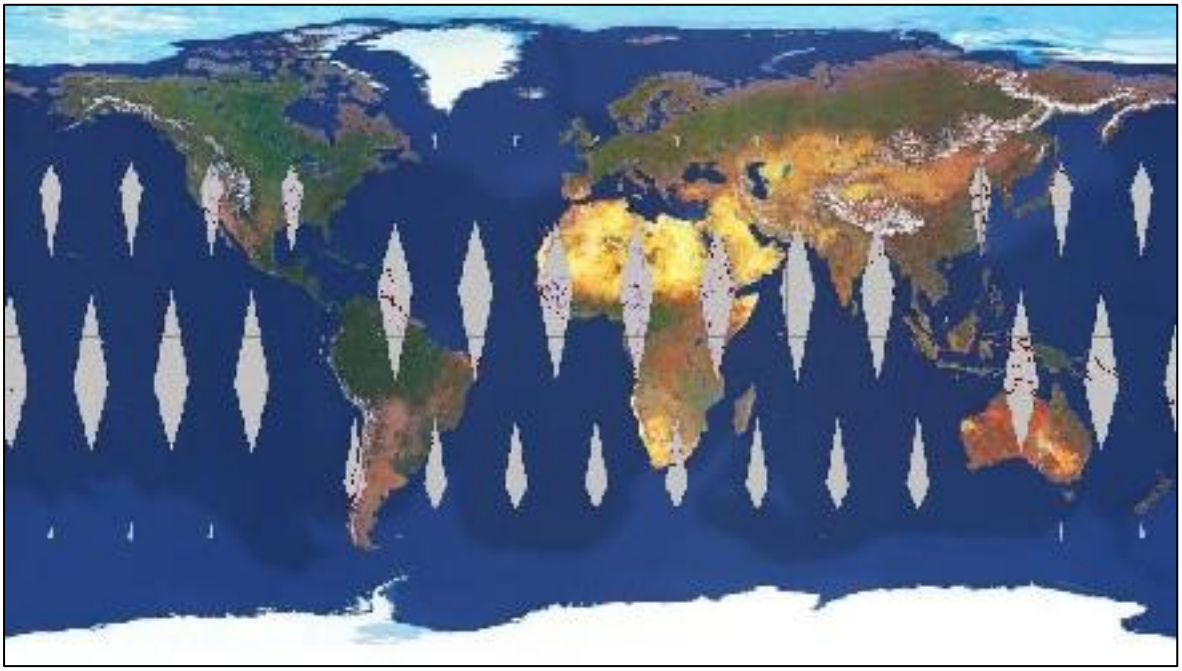

Figure 1. A Map of a Typical Day of Coverage with 28 half-orbits

1.2.2 Resolution

Data are resampled to spatial resolutions ranging from 5.4 km to 56 km. The sampling interval at the Earth's surface is 10 km for all channels. The 89.0 GHz channel also contains data sampled to 5 km. Please see 89 GHz Scan Spacing for a figure that illustrates A and B scan interleaving.

All channels are available at an unsampled Level-1B resolution. The higher-resolution channels are resampled to correspond to the footprint sizes of the lower-resolution channels. The Level-2A

algorithm spatially averages the multiple samples of the higher-resolution data into the coarser resolution Instantaneous Field of View (IFOV) of the lower-resolution channels with the Backus-Gilbert method. The resulting brightness temperatures are called effective observations in contrast to the original or actual observations. The following table summarizes these relationships (Marquis et al. 2002):

Table 5. Spatial Characteristics of Observations

Resolution	Footprint size	Mean spatial resolution	Channels					
			89.0 GHz	36.5 GHz	23.8 GHz	18.7 GHz	10.7 GHz	6.9 GHz
1	75 km x 43 km	56 km	•	•	•	•	•	• o
2	51 km x 29 km	38 km	•	•	•	•	• o	
3	27 km x 16 km	21 km	•	•	• o	o		
4	14 km x 8 km	12 km	•	o				
5	6 km x 4 km	5.4 km	o					

• Includes Level-2A (smoothed) data
o Includes Level-1B (un smoothed) data at original spatial resolution

1.3 Temporal Information

1.3.1 Coverage

Each swath spans approximately 50 minutes. The number of satellite passes per day is a function of latitude as shown in AMSR-E Observation Times.

See the AMSR-E web page for a summary of temporal coverage for different AMSR-E products and algorithms.

1.3.2 Resolution

The data sampling interval is 2.6 msec for each 1.5-sec scan period for the 6.9 GHz to 36.5 GHz channels, and 1.3 msec for the 89.0 GHz channel. AMSR-E collects 243 data points per scan for the 6.9 GHz to 36.5 GHz channels, and 486 data points for the 89.0 GHz channel.

2 DATA ACQUISITION AND PROCESSING

2.1 Acquisition

Please refer to the AMSR-E Instrument Description document. AMSR-E/Aqua L1A Raw Observation Counts are used as input to calculating the Level-2A brightness temperatures.

2.2 Processing

2.2.1 Derivation Techniques and Algorithms

The objective of the Level-2A algorithm is to bring the Level-1A antenna temperatures to a set of common spatial resolutions using a set of weighted coefficients. The algorithm resamples Level-1A antenna temperatures and converts them to Level-2A brightness temperatures.

The resampled antenna temperature (T_{ac}) is defined as a weighted sum of observed antenna temperatures (T_{ai}):

$$T_{ac} = \sum_{i=1}^{N} a_i \, T_{ai}$$

Equation 1

Where:

a_i = weighting coefficients

Antenna temperature observations are corrected for cold-space spillover and cross-polarization effects to obtain brightness temperatures averaged over the normalized crossover-polarization antenna pattern. The observed brightness temperatures (Tbi) are expressed as:

$$T_{bi} = \int Tb(\rho)\, Gi(\rho)\, dA \qquad [2]$$

Equation 2

Where:

$T_b(\rho)$ = brightness temperature at location ρ

$G_i(\rho)$ = antenna gain pattern corresponding to the specific observation

Antenna temperature coefficients, effective hot load temperatures, calibration counts, and antenna coefficients are only provided for users who want to see how brightness temperatures were calculated for this data set. They are not required to view brightness temperatures.

Each Level-2A (effective) observation within a single instrument scan is calculated using coefficients that describe the relative weights of the neighboring Level-1A (actual) observations. Coefficients are unique for every position along the instrument scan, yet they do not vary from scan to scan. The Backus-Gilbert method produces the weighting coefficients for Level-1A data. Antenna patterns and relative geometry are known a priori, allowing weighting coefficients to be calculated before observations are collected. Although the Backus-Gilbert method can, in principle, be used to construct effective observations corresponding to gain patterns either smaller or larger than those in the actual observations, the noise amplification from smaller gain patterns (deconvolution) is typically very high.

Calculation of weighting coefficients requires specification of the shape of the target pattern, the location of the target pattern relative to the actual measurements, the set of actual observations used, and the smoothing parameter for each constructed observation. Actual observations within an 80 km radius of the constructed pattern are considered for possible contributors to the construction. Observations that are too far from the target pattern to play a role in the construction are assigned a weight of zero by the algorithm. Weighting coefficients are computed based on a simulation of the antenna patterns for a portion of a circular orbit around a spherical earth.

The smoothing factor at each point across the scan of each Level-2A data set is chosen in the following way: The algorithm applies the same amount of smoothing at the center to observations close to the edges. This ensures that noise decreases as the spatial density of the actual observations increases toward the edges. For construction of observations at the extreme edges, sufficient smoothing is added to keep noise at the edges from exceeding the noise at the center. For a given Level-1A channel, noise decreases as the resolution of the constructed pattern becomes larger, and the number of useful actual observations increases (Ashcroft and Wentz 2000).

2.2.2 Processing Steps

The algorithm reads an entire file (one half orbit) of Level-1A data at a time and uses calibration coefficients to convert antenna temperatures to brightness temperatures. Coefficients embedded in the data are discarded, and new values are calculated. The algorithm applies weighting coefficients from a table of values to resample the Level-1A data using Equation 1. The weighting coefficients corresponding to each constructed observation are stored as a 29 x 29 array, which applies weights to actual observations ± 14 scans and ± 14 locations along the scan from the constructed observation. Most of the coefficients in the array are zero. In an ideal case, weighting coefficients

are applied to each corresponding constructed target pattern within the scan. Level-1A data produce unsmoothed Level-1B brightness temperatures and smoothed Level-2A brightness temperatures using Equation 2 (Ashcroft and Wentz 2000).

2.3 Quality, Errors, and Limitations

2.3.1 Quality Assessment

Each HDF-EOS file contains core metadata with Quality Assessment (QA) metadata flags that are set by the Science Investigator-led Processing System (SIPS) at the Global Hydrology and Climate Center (GHCC) prior to delivery to NSIDC. A separate metadata file with an .xml file extension is also delivered to NSIDC with the HDF-EOS file; it contains the same information as the core metadata. Three levels of QA are conducted with the AMSR-E Level-2 and -3 products: automatic, operational, and science QA. If a product does not fail QA, it is ready to be used for higher-level processing, browse generation, active science QA, archive, and distribution. If a granule fails QA, SIPS does not send the granule to NSIDC until it is reprocessed. Level-3 products that fail QA are never delivered to NSIDC (Conway 2002). Only a QA file is produced when there are no L-2A brightness temperature data that qualify for retrieval.

2.3.2 Automatic QA

RSS generates AMSR-E Level-2A files from Level-1A files supplied by the Japan Aerospace Exploration Agency (JAXA). The Level-2A data files contain data flags set by JAXA for the Level-1A files and flags set by RSS. RSS quality assessment is performed when Level-2A files are generated. Resampled observations are generated wherever a valid Level-1A observation exists. This occurs when the Level1A_Scan_Chan_Quality_Flag is acceptable, and the actual observation at that location is within a plausible range. If neighboring observations are not acceptable, either because the entire neighboring scan is not acceptable, or because particular observations are implausible, the weights corresponding to the remaining acceptable observations are renormalized in order to calculate the resampled observation.

2.3.2.1 JAXA Data Quality Flags

The Data_Quality element contains the primary JAXA data quality flags. Aside from this element, JAXA provides additional quality information through reserved data values. For example, -9999 counts indicate missing data. RSS does not use the JAXA Data_Quality data element in Level-2A processing, but this element is included in the Level-2A data set for the benefit of other users.

2.3.2.2 RSS Quality Assessment

RSS adds three types of quality assessment indicators for each scan:

- 4-Byte Scan_Quality_Flag
  - Identical flag repeated for the Low Swath, High 89A Swath, and High 89B Swath
- 2-Byte Channel_Quality_Flag for each channel
  - 10 channels for the Low Swath
  - channels for the High 89A Swath
- 2 channels for the High 89B Swath
  - 2-Byte Resampled_Channel_Quality_Flag for each resampled channel
  - 30 channels for the Low Swath

The summary bit 0 of the Channel_Quality_Flag is automatically set whenever any of the bits in the Scan_Quality_Flag are set. Thus, the user can determine whether the data are useable by examining only the Channel_Quality_Flag without examining the Scan_Quality_Flag.

2.3.2.3 Scan_Quality_Flag

A Scan_Quality_Flag is provided for each scan. These flags pertain to all observations of a scan including all Level-1A and resampled channels.

Table 6. Summary of Scan_Quality_Flag

Bit	Meaning	Value = 0	Value = 1	Description
0	Summary Flag	All higher bits are equal to zero	Otherwise	The Scan Summary bit captures the conditions of all the other bits in the Scan_Quality_Flag. It is set to one if any of the bits 2 through 31 are set. The summary flag does not describe those characteristics that apply to a single channel.
1	Antenna Spin Rate	Within range	Missing or out of range	Bit 1 is set if the antenna spin rate is out of range, which is defined as 4.167 percent from nominal.
2	Navigation	Within range	Missing or out of range	Bit 2 is set if the position or velocity of the navigation data for that scan is out of bounds. The bounds are 6500-8000 km from the Earth's center to the satellite and 4-10 km/sec for spacecraft velocity. Note that these bounds are extremely large, and this flag is intended to identify bogus data rather than real anomalies in the navigation.

Bit	Meaning	Value = 0	Value = 1	Description
3	RPY Variability	Within range	Out of range	Bit 3 is set if the roll, pitch, or yaw variability from scan to scan is out of bounds. Only Midori-2 AMSR has this problem. A scan-to-scan variation in either roll, pitch, or yaw that exceeds 0.05 degrees is considered out of bounds.
4	RPY	Within range	Out of range	Bit 4 is set whenever the roll, pitch, or yaw exceeds 2.0 degrees.
5	Earth Intersection	All on earth	Some not on Earth	Bit 5 is set if any of the observation locations fail to fall on the Earth. This occurs during large orbit maneuvers.
6	Hot Load Thermistors	Within range	Missing or out of range	Bit 6 is set whenever the thermistors on the AMSR hot load are out of bounds, which is defined as their rms variance being greater than 10K or any single thermistor being outside the range 283.17K - 317.16K for AMSR-E and 285.17K - 316.94K for Midori-2 AMSR. When these temperature limits are converted to thermistor counts, they correspond to the minimum and maximum allowable count values.
7-31	Not Used, Always 0	N/A	N/A	N/A

2.3.2.4 Channel_Quality_Flag

All flags in this data element are set in response to characteristics of the calibration measurements for a specific AMSR channel. In general, calibration measurements (hot and cold) are averaged over adjacent scans to compute the antenna temperatures from raw counts. The default process is to average calibration counts over a range from one scan before the scan to one scan after the scan although only a subset of these calibration measurements is used if some are unacceptable. The Calibration Quality Flags are set on the basis of the same calibration measurements over which the calibration averaging is performed. See the Calibration section of the AMSR-E Instrument Document for details of AMSR-E calibration. Also, it is important to note that the flag called Level1A_Scan_Chan_Quality_Flag was replaced by three new flags:

- Channel_Quality_Flag_6_to_52 for Low_Res_Swath
- Channel_Quality_Flag_89A for High_Res_A_Swath
- Channel_Quality_Flag_89B for High_Res_B_Swath

Table 7. Summary of Channel Quality Flag

Bit	Meaning	Value = 0	Value = 1	Description
0	Summary Flag	Good	Questionable or bad	Bit 0 is a summary flag. This bit is set if any of the bits 2 through 15 are set. Note that bit 11 is set if any of the geolocation error bits in the Scan_Quality_Flag are set. Hence, if any errors are reported by the Scan_Quality_Flag, Bit 0 of all Channel_Quality_Flags is set to 1.
1	T_bAvailability	Yes	No	Bit 1 indicates whether Level-2A brightness temperatures are computed for this channel. When there are severe problems, as indicated by any of the bits 2, 3, 4, or 12 being set, no brightness temperatures is computed and bit 1 is set to 1.
2	Scan Number	Not first or last scan	First or last scan	Bit 2 is set for the first and last scans of each Level-2A file. Because the calibration and quality checking of each scan uses both the adjacent scans, the calibration and quality checking can not be performed on the first and last scan of the file.
3	Serious Calibration Problem	No, all is good	Yes	Bit 3 is set if one of the following occurs: 1.The automatic gain control has changed from either the preceding or succeeding scan. 2.The receiver automatic gain control is out of bounds. 3.All calibration counts for either or both the hot load and cold sky are out of bounds.
4	Hot-cold Counts Check 1	> 0	<= 0	Bit 4 is set if the cold calibration counts are the same or greater than the hot calibration counts.
5	Thermistors	Within bounds	Out of bounds	Bit 5 is set if the hot load thermistors are out of range. The acceptable range for the thermistors is described above for bit 6 of the Scan_Quality_Flag.
6	T_{eff} Type	Dynamic T_{eff}	Static T_{eff}	Bit 6 equals 0 denotes that the dynamic T_{eff} is used. This is the usual condition. Bit 6 equals 1 denotes that the static T_{eff} is used, which should rarely if ever occur.
7	No.of Cold Counts	>= 8	< 8	Bit 7 is set if there are fewer than 8 cold counts that are in bounds.

Bit	Meaning	Value = 0	Value = 1	Description
8	No. of Hot Counts	>= 8	< 8	Bit 8 is set if there are fewer than eight hot counts that are in bounds.
9	Hot-cold Counts Check 2	>= 100	< 100	Bit 9 is set if the difference between hot and cold counts is less than 100.
10	Hot-cold Counts Check 3	>= Channel minimum	< Channel minimum	Bit 10 is set if the difference between hot and cold counts is less than a channel-dependent threshold.
11	Geolocation	No problem exists	Problem exists	Bit 11 is set if there is a geolocation error as reported by the Scan_Quality_Flag.
12	T_{eff}availability	Yes	No	Bit 12 is set to 1 if T_{eff} is not available. This should rarely if ever occur.
13-15	Not Assigned, Always 0			

2.3.2.5 Resampled_Channel_Quality_Flag

A Resampled_Channel_Quality_Flag is provided with the L2A data, but it is redundant with the Channel_Quality_Flag and does not usually need to be used. For the lower frequency channels, the first two bits (0 and 1) of the Channel_Quality_Flag are copied to the first two bits of the corresponding Resampled_Channel_Quality_Flag. For the 89A Channels, the first two bits (0 and 1) of the Channel_Quality_Flag are copied to the first two bits of the corresponding Resampled_Channel_Quality_Flag. For the 89B Channels, the first two bits (0 and 1) of the Channel_Quality_Flag are copied to bits 2 and 3 of the corresponding Resampled_Channel_Quality_Flag.

Table 8. Resampled_Scan_Chan_Quality_Flag

Bit	Meaning
0-1	Equal to corresponding bits of corresponding channels
2-15	Not assigned

Before working with any channel of data, users should confirm that both the Scan_Quality_Flag and the Channel_Quality_Flag indicate that the scan is acceptable.

2.3.3 Operational QA

AMSR-E Level-2A data arriving at GHCC are subject to operational QA prior to use in processing higher-level products. Operational QA varies by product, but it typically checks for the following criteria in a given file (Conway 2002):

- File is correctly named and sized
- File contains all expected elements
- File is in the expected format
- Required EOS fields of time, latitude, and longitude are present and populated
- Structural metadata is correct and complete
- The file is not a duplicate
- The HDF-EOS version number is provided in the global attributes
- The correct number of input files were available and processed

2.3.4 Science QA

AMSR-E Level-2A data arriving at GHCC are also subject to science QA prior to use in processing higher-level products. If less than 50 percent of a granule's data is good, the science QA flag is marked suspect when the granule is delivered to NSIDC. In the SIPS environment, the science QA includes checking the maximum and minimum variable values, the percentage of missing data, and out-of-bounds data per variable value. At the Science Computing Facility (SCF) and also at GHCC, science QA involves reviewing the operational QA files, generating browse images, and performing the following additional automated QA procedures (Conway 2002):

- Historical data comparisons
- Detection of errors in geolocation
- Verification of calibration data
- Trends in calibration data
- Detection of large scatter among data points that should be consistent

Geolocation errors are corrected during Level-2A processing to prevent processing anomalies such as extended execution times and large percentages of out-of-bounds data in the products derived from Level-2A data.

The Team Lead SIPS (TLSIPS) developed tools for use at SIPS and SCF for inspecting the data granules. These tools generate a QA browse image in Portable Network Graphics (PNG) format and a QA summary report in text format for each data granule. Each browse file shows Level-2A and Level-2B data. These are forwarded from RSS to GHCC along with associated granule information where they are converted to HDF raster images prior to delivery to NSIDC.

Please refer to the AMSR-E Validation Data for information about data used to check the accuracy and precision of AMSR-E observations.

2.3.5 Error Sources

The Level-2A data set includes unsmoothed Level-1B data derived from antenna temperatures. See the AMSR-E Instrument Description Web page for a description of the error sources associated with radiometer calibration.

Error on a constructed brightness temperature observation arises from two sources. The first source of error is a mismatch between the ideal antenna pattern and the construction, and the second is random measurement error. The variance of a constructed brightness temperature is independent of the actual temperature field, depending only on the weighting coefficients and the observation error of each observed brightness temperature. The effect of random measurement error is more easily quantified than the effect of fit error. Increased smoothing reduces the noise factor but degrades the fit. This tradeoff is most noticeable at the edges of the scan. Fit and noise factor near the center of the scan are optimized for fit. See the Derivation Techniques and Algorithms section of this document for more information. As a result of the spatial averaging that produces the Level-2A data, errors of neighboring observations within any single channel are somewhat correlated. Errors between channels are not correlated in any case. While the Level-2A data set is well-suited for applications that require a combination of multiple channels of observations, the user should recognize that errors on observations within a single channel are not necessarily independent (Ashcroft and Wentz 2000).

2.3.6 Along-Scan Error

An along-scan error is caused by AMSR-E's cold mirror or warm load entering the FOV of the feedhorns, or by the main reflector seeing part of the spacecraft. The RSS performed an analysis of the AMSR-E along-scan error and developed a correction.

In spite of RSS's best efforts to accomplish a robust AMSR-E along-scan temperature correction, users should note that some contamination remains in the 14 pixels at the beginning of each scan line. Users should determine whether to include those pixels based on their specific research application and the effects of the contamination described below.

In early 2007, researchers at NSIDC conducted an along-scan error analysis by examining brightness temperature distributions for each sample position in three different, relatively uniform climatic regions over a sufficiently long time period to eliminate effects from random, transient events. The three regions included a portion of Antarctica, an area of the Indian Ocean south of Australia, and an area of African jungle in the Salonga National Park region of the Democratic Republic of the Congo.

NSIDC concluded that even after the RSS along-scan correction, a significant cold bias remains in brightness temperature measurements in all channels over Antarctic regions from the beginning of

each scan line. There is also some evidence of a cold bias in 7 GHz channels over jungle areas. There does not appear to be a bias in any channels observing ocean areas.

2.3.7 Along-scan Error Analysis and Applied Correction Made by RSS

To determine the magnitude of this effect at the swath edges, RSS computed the difference between the AMSR-E antenna temperature and the radiative transfer model. This difference was plotted versus along-scan cell positions in Figure 2, where the antenna temperature differences have been averaged over the first year of AMSR-E operation. The cell positions go from 1 to 243. The antenna temperature differences are shown for all 14 AMSR-E channels. Each channel is color-coded and is offset by 1 K so that the results can be easily visualized. The straight horizontal lines in Figure 2 are the zero reference lines. The spacing between the horizontal lines is 1 K.

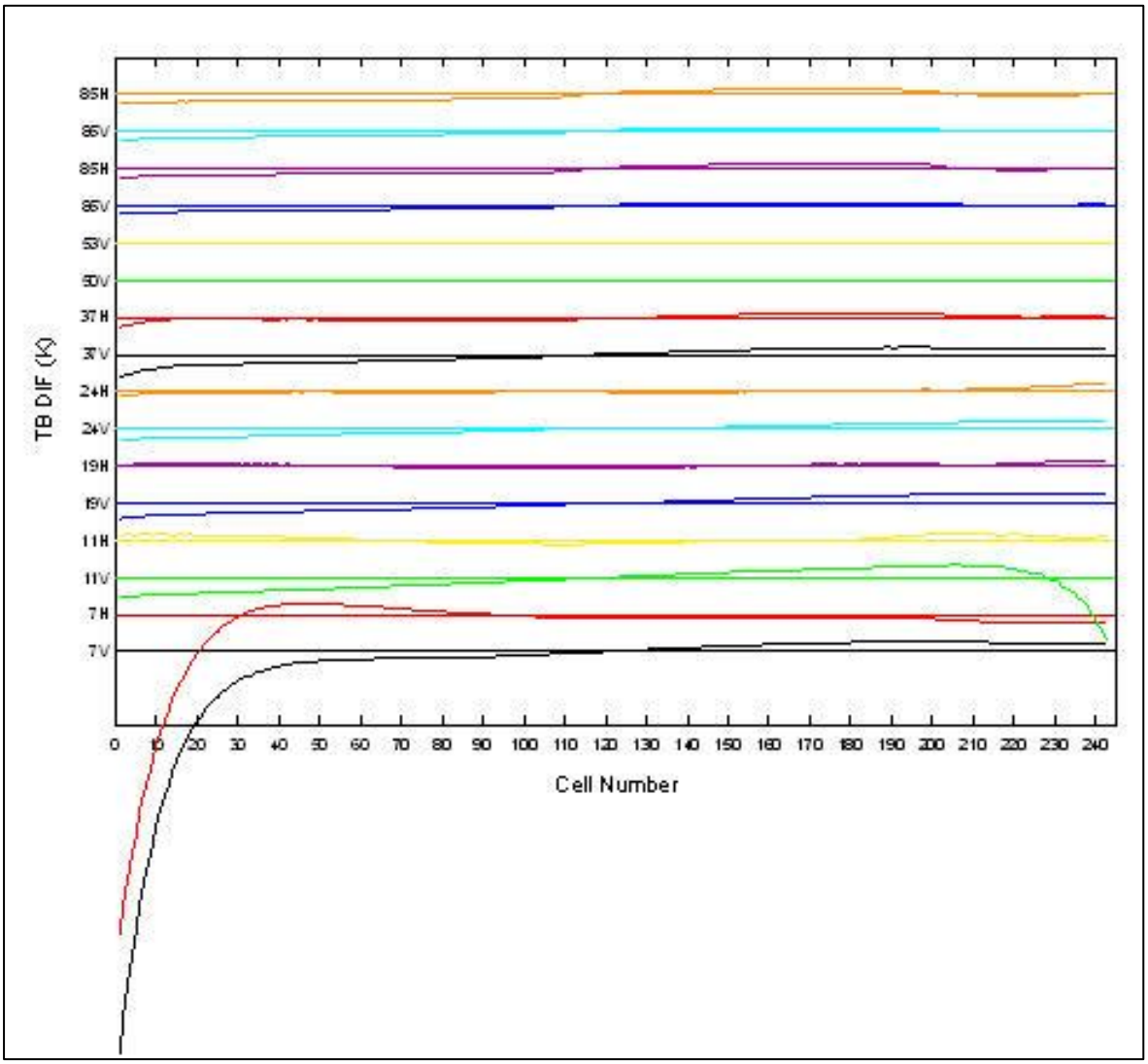

Figure 2. Along-scan Error in AMSR-E Observation

In general, most channels show little along-scan variation. However, there are three channels (7 GHz v-pol, 7 GHz h-pol, and 11 GHz v-pol) that show a significant cold bias at the swath edges. Some of the other channels exhibit similar but smaller behavior. The most affected is the 7 GHz v-pol which has a cold bias of about 10 K at the beginning of the scan.

Based on the results shown in Figure 2, a correction table was made. This table provides an antenna temperature adjustment for each AMSR-E channel that is a function of the along-scan cell position. This adjustment eliminates the along-scan error in the mean sense. RSS repeated this analysis and stratified the data into two half-year time periods and into two orbit segments (ascending and descending). The variation in the along-scan error for these four stratifications is about 0.1 K, thereby showing the along-scan error is a constant feature. This along-scan adjustment was implemented into the standard AMSR-E processing algorithm. However, some caution should still be exercised when using pixels 1-14 for the 7 GHz channel for which there may be some residual along-scan error.

2.3.8 Position-in-Orbit Description

The AMSR-E Level-2A product follows the granule conventions designed and set in L-1A. Each file provides some overlap to the previous and next file. This supports the ability to do 1 to 1 file processing. The overlap provides each granule with a ~10 scan look into the forward and backward neighboring files.

This ~10 scan overlap at the edges of the file belongs with the neighboring files, and eliminates the need to open and read the files before and after the file in use. When deciding which portion of the overlap to use, choose the half of the overlap that is contiguous with the swath in the file and ignore the overlap at the edge of the file.

2.3.9 Sensor Error Information

2.3.9.1 Geolocation

A misregistration relative to coastlines and other land features was recognized in the AMSR-E brightness temperature imagery. The error in geolocation was about 5 - 7 km and was due to a misalignment of the AMSR-E sensor relative to the spacecraft. The problem was fixed by a trial-and-error method in which various roll, pitch, and yaw corrections were applied to the AMSR-E alignment until proper registration was obtained.

A separate geolocation analysis was done for each channel, which showed that for a given frequency the v-pol and h-pol channels are well aligned. Furthermore, the 19, 23, and 37 GHz Channels are also well aligned with each other. Corrections to the geolocation for Channels 19 GHz through 89 GHz were implemented in Version B06 algorithm.

In Version B07, the 7 and 11 GHz Channels were resampled to match the locations of the higher frequencies since it was determined that the 7-GHz and 11-GHz horns are pointing in a slightly different direction than the 19, 23, and 37 GHz horns. This required re deriving the sampling weights with the center of the target cell positioned at the location of the 19 GHz Channel rather than at the 7 or 11 GHz footprint position. One drawback is that the un-resampled 7 and 11 GHz observations are missing an exact specification of latitudes and longitudes.

2.4 Calibration

AMSR-E's calibration system has a cold mirror that provides a clear view of deep space (a known temperature of 2.7 K) and a hot reference load that acts as a blackbody emitter; its temperature is measured by eight precision thermostats. After launch, large thermal gradients due to solar heating developed within the hot load, making it difficult to determine from the thermostat readings the average effective temperature, or the temperature the radiometer sees.

2.4.1 BEFORE 07 JANUARY 2005 (B01 AND B02 ALGORITHMS)

Remote Sensing Systems (RSS) used coincident Tropical Rainfall Measuring Mission (TRMM) Microwave Imager (TMI) and Special Sensor Microwave/Imager (SSM/I) satellite data over oceans to estimate the effective hot load temperature. A radiative transfer model used these data to compute the intensity of radiation entering the feedhorns. The model took into account different view geometries and channel differences between AMSR-E, SSM/I, and TMI. This process essentially provided earth-target calibration points, which were combined with the cold mirror temperature to compute a two-point linear extrapolation that yielded the hot load effective temperature for 10.7 to 89 GHz.

2.4.2 BEFORE MARCH 2006 (B03 THROUGH B06)

To estimate the effective hot load temperature, RSS assumed that the effective temperature is independent of channel polarization and then used climatic cloud and water vapor data along with daily SST and NCEP winds, to define the effective temperature as a function of the observed polarization differences.

2.4.3 AFTER MARCH 2006 (B07 AND NEWER ALGORITHMS)

2.4.3.1 Computing the Effective Temperature of the AMSR-E Hot Load

An on-orbit calibration is required for AMSR-E because of a design flaw in the AMSR-E hot load. For the initial method, the effective temperature of the AMSR-E hot load was estimated using SSM/I and TMI, sea-surface temperature (SST), wind, vapor, and cloud water observations.

Although the old method of computing Teff worked well, it created a dependency on the SMM/I and TMI observations which could delay processing. Thus, a hot load calibration procedure that did not rely on other satellites was desirable.

The primary reason SSM/I and TMI were required was to specify the water vapor and cloud water. The other two relevant parameters, SST and wind, can be obtained with sufficient accuracy from NCEP Final Analysis fields. To remove the dependence on the SSM/I and TMI vapor and cloud retrievals, modifications were made to the way in which the effective temperature is computed. The new method is based on the assumption that the effective temperature does not depend on polarization, for example, it is the same for v-pol and hâ€“pol. This assumption seems to be valid based on both empirical data (v-pol and h-pol effective temperatures coming from the SSM/I-TMI method are similar) and physical considerations (hot-load is an unpolarized source). Under this assumption, the method can be modified to make it insensitive to the specification of vapor and cloud.

The first step of the process is to estimate the value of Effective Temperature (Teff) for each AMSR-E observation. The following expression is used to estimate the effective temperature

$$T_{eff\ i} = T_c + \rho_i (T_{Ai,rtm} - T_c)$$

Equation 3

Where:

T_C is the brightness temperature for the cold space observation

$T_{Ai,rtm}$ is the antenna temperature computed from the RTM given the ancillary information such as SST, wind, vapor, and cloud.

The subscript i denotes AMSR channel.

The term ρ_i is the following ratio of the radiometer counts

$$\rho_i = \frac{C_{Hi} - C_{Ci}}{C_{Ei} - C_{ci}}$$

Equation 4

Where:

subscripts C, H, and E denote cold-space counts, hot-load counts, and earth-viewing counts, respectively.

Equation 3 is a linear extrapolation based on the cold-calibration point and the earth-calibration point.

The next step is to form a linear combination of effective temperatures that are relatively insensitive to variations in vapor, cloud, and to some degree wind. For a given frequency, this linear combination of Teff is represented by the following equation:

$$\hat{T}_{eff\ j} = [1 - \Lambda(W)] \sum_{i=1}^{10} p_{ij} T_{eff\ i} + \Lambda(W) \sum_{i=1}^{10} q_{ij} T_{eff\ i}$$

Equation 5

Where:

subscript j denotes channel frequency, pij and qij are static regression coefficients

W is wind speed. The summations are over the 10 AMSR channels from 7 to 37 GHz. However, a slightly modified version is used for the 89 GHz Channels. The function ∧(W) smoothly goes from 0 to 1 as the wind speed goes from 3 to 11 m/s. Thus, the first term in Equation 5 corresponds to low-to-moderate winds, and the second term corresponds to moderate-to-high winds. Two wind speed terms are used because the wind speed response of the RTM is highly non-linear. The wind speed value comes from NCEP Final Analysis fields.

The regression coefficients pij and qij are found from computer simulations so as to minimize the error in the estimation of effective temperature due to variations in wind, vapor, and cloud. The method for finding the coefficients is similar to that used to find the regression coefficients for the geophysical retrieval algorithms. In essence, Equation 5 is an algorithm for estimating the hot load effective temperature.

The next step is to correlate $\hat{T}_{eff\ j}$ with the thermistor temperatures and orbit position. This is done by using the following expression:

$$\hat{T}_{eff\ j} = a_{0j} + b_{0j} \sin \propto + c_{0j} \sin 2 \propto + \sum_{k-1}^{8} a_{kj} (T_k - 303) \sin \propto + c_{kj} (T_k - 303) \sin 2 \propto$$

Equation 6

Where:

subscript k denotes the eight hot-load thermistors

T_k are the thermistor temperatures

α - 90 degrees is the orbit position angle relative to the ascending node crossing of the ecliptic plane.

There are 27 regression coefficients to be found for each frequency: a_{kj}, b_{kj}, and c_{kj}. These regression coefficients are allowed to vary in time. A ±150 orbit moving time window is used to specify the coefficients. The weighting function for the time window is triangular, going to zero at 150 orbits before the current orbit and 150 orbits after the current orbit. Thus, the time scale for the variation in the a_{kj}, b_{kj}, and c_{kj} coefficients is approximately 10 days.

There are three additional improvements that were implemented. The first relates to the SSTs that were used to specify $T_{Ai,rtm}$. The SST values come from Reynolds' weekly Optimum Interpolation (OI) SST product. Since this SST product is a weekly value, it does not include any diurnal components. For the AMSR-E early afternoon orbit, diurnal variations in SST can be large when there are light winds. Accordingly, a diurnal adjustment is applied to the OI SST model the diurnal variability of SST.

The last improvement is to apply a smoothing function to the estimation of the radiometer gain, which is given by the following equation

$$G = \frac{\hat{T}_{eff\ j} - T_c}{C_{Hi} - C_{ci}}$$

Equation 7

The gain is expected to vary smoothly over the orbit. Random errors in the estimation of $\hat{T}_{eff\ j}$ shows up as rapid variations in G. A smoothing function is applied to G to remove the variability on short time scales (minutes), thereby further reducing the error in the estimation.

2.4.3.2 Recalibration of AMSR-E Hot Load and Along-Scan Adjustments

The correction of the AMSR-E geolocation problems required that the AMSR-E sensor alignment be rolled relative to the spacecraft frame by 0.09 degrees. Changing the roll of the sensor results in

a change in the incidence angle. With this roll adjustment, the true incidence angle was found to vary across the swath contrary to the assumption that it was nearly constant. This modification of the incidence angle has small but significant effects on the AMSR-E calibration. The calibration is based on measurements of the ocean surface, and the emission from the ocean surface varies with incidence angle. To address the change in incidence angle, AMSR-E was completely recalibrated and a new hot load effective temperature table was found. The along-scan antenna temperature adjustment was also recalculated using the new roll angle Thus, the along-scan errors in the antenna temperatures are significantly reduced except near the swath edge where the cold mirror interferes with the field of view.

Earth incidence angle is computed and included in Level-2A files in data field Earth_Incidence. These variable earth incidence angle data should be used appropriately, especially for geophysical retrievals depending upon incidence angle. Using the previously assumed constant incidence angle will likely result in along scan bias. The Level-2A Brightness Temperature data set is intended to be a faithful representation of the brightness temperatures observed by the instrument. Thus, due to the sensor-to-spacecraft roll, incidence angle is variable along scan, and brightness temperatures are correspondingly variable along scan. This along scan variability in observed brightness temperatures is not removed and should be accounted for by using the computed Earth_Incidence.

2.4.3.3 Implementation of Flagging Algorithm for RFI from Geostationary TV Satellites

As part of the SST and wind validation activity, anomalous retrievals were found off the West Coast of Europe and in the Mediterranean Sea. After some investigation, these erroneous retrievals were determined to be due to Radio Frequency Interference (RFI) from a European satellite TV service. ASMR-E is receiving the broadcast from two European geostationary satellites that operate near the 10.7 GHz band. The satellite TV signal is reflecting off the ocean surface into the AMSR-E field of view. AMSR-E bandwidth at 10.7 GHz is 100 MHz, whereas the protected band is only 20 MHz. The TV signal is coming from the unprotected part of the 100-MHz band.

The TV RFI was determined to be coming from two satellites: one positioned at a longitude of 13 degrees E above the equator and the other at 19 degrees E. An algorithm was developed that computes the angle between AMSR-E look vector and the specular reflection vector for the TV RFI. This angle is called the RFI angle. Small RFI angles correspond to cases in which the TV RFI is being reflected off the ocean surface directly towards AMSR-E.

When the RFI angle is less than 12 degrees, in general the observation should be flagged as RFI contaminated. However, in the North Sea, the RFI is particularly strong. For this region, an RFI angle of 17 degrees is the threshold.

2.4.3.4 Correction for August-September 2003 Aqua Pitch Error

An anomaly occurred between 12 August 12 and 6 September 2003 due to an error in knowledge of the spacecraft pitch. In the Level-1A data, the definitive ephemeris was used for this period so the geolocation values are correct. However, the fact that the anomaly caused Aqua to be inadvertently pitched during this time period was not accounted for in the Level-1A data. In the Level-2A algorithm, the satellite pitch anomaly during this period was modeled as a ramp function and corrected.

2.4.3.5 Correction for Lunar Radiation Entering the AMSR-E Cold Mirror

Twice each month the moon enters the Field of View (FOV) of the AMSR-E cold mirror. The moon's surface temperature varies from 120 K night to 370 K day and has a relatively high emissivity. As a result, the moon acts as a source of contamination to the cold sky measurement.

A correction was applied to remove the lunar contamination. The correction depends upon the following factors:

1. The angle between the vector going from the satellite to the moon and the boresight vector of the cold mirror. This is the dominant term. When this angle becomes small, a few degrees or less, lunar contamination becomes significant. This angle is called the lunar angle.
2. The phase of the moon. A full moon is hotter than a new moon and hence has a higher brightness temperature.
3. The distance from the satellite to the moon. Radiation intensity falls off as the inverse of the square of the distance.

The lunar antenna temperature contribution to the cold sky observations is computed and then is scaled in terms of cold counts. The lunar cold counts are subtracted from the AMSR-E cold count observations to obtain a cold count value free of lunar contamination. For the case of 89 GHz, when the lunar angle is less than one degree, the lunar contamination is too large to perform the correction and these observations are flagged as bad and are not processed. The excluded observations are extremely rare. The accuracy of this correction is estimated to be in the order of 0.1 K.

2.4.3.6 Adjustment to Match the 89A and 89B Observations During Resampling

When the 89 GHz Channels are resampled to lower spatial resolutions, the observations from the A-horn and the B-horn are combined. However, the incidence angles for these two horns are different with the B-horn incidence angle being about 0.6 degrees smaller than the A-horn. To compensate for the difference in incidence angle, the following adjustments were made to the A-horn measurements before resampling.

$$T_{AV,adj} = 0.130671 + 0.99325T_{AV}$$

Equation 8

$$T_{AH,adj} = 0.472994 + 0.992742T_{AH}$$

Equation 9

These expressions were found from doing linear regression of actual A-horn and B-horn observations over the first two mission years of AMSR-E. The application of these equations normalizes the A-horn measurements to the B-horn incidence angle.

2.4.3.7 Implementation of using UT1 time to compute the Earth rotation angle.

Aqua's position, velocity, and attitude vectors are given in terms of the J2000 inertial coordinate system. To compute Earth latitudes and particularly longitudes, it is necessary to compute the Earth rotation relative to the J2000 systems. The proper calculation requires using the UT1 time, which can be as much as one second different from UTC time. To obtain UT1, the Level-2A algorithm accesses the U.S. Naval Observatory database each day to obtain the current UT1. One advantage of this procedure is that it is independent of leap seconds; therefore, there is no discontinuity in the geolocation parameters when a leap second occurs.

2.4.3.8 Intercalibration with SSM/I F13 and WindSat

F13 and WindSat provide a backbone of consistent long-term observations, relatively free from diurnal effects. Local observation times for F10, F11, F14, F15, and F16 all drift by two to six hours over the years, so these instruments have been measuring a continuously differing viewpoint in Earth's diurnal cycle. The larger the diurnal drift, the more challenging it is to distinguish from sensor drift. AMSR-E is in a stable orbit on Aqua, so diurnal drift is not a problem. However, AMSR-E observes local times of 1:30 a.m./p.m.; AMSR-E day and night passes observe significantly more pronounced diurnal variations than F13 and Windsat passes at approximately 6:00 a.m./p.m.. For more information about intercalibration choices and methodology, please refer to the RSS Crossing Times Web page.

2.5 Instrumentation

2.5.1 Description

Please refer to the AMSR-E overview page.

3 SOFTWARE AND TOOLS

For tools that work with AMSR-E data, including the AMSR-E Swath-to-Grid Toolkit, see the AMSR-E web page.

4 VERSION HISTORY

Changes to this algorithm include:

Complete recalibration to RSS Version 7 standard, as follows:

- Intercalibration with other microwave radiometers, particularly SSM/I F13 and WindSat
- Calibration with improved Radiative Transfer Model (RTM): RSS RTM Version 2011
- Updated ocean emissivity model (Meissner and Wentz 2012)
- Adjustment of the water vapor and oxygen absorptions, particularly the water vapor continuum absorption
- Improved calibration over land, based on heavily vegetated tropical rainforest scenes
- Nonlinearity correction at 18.7 GHz, brightness temperatures approx. 2 degrees K lower over land
- Adjustment to Antenna Pattern Coefficients (APC) for cross-polarization and spillover
- Slight shift to the 18.7 GHz center observation frequency
- Adjustment of effective hot-load temperature

Improved Radio Frequency Interference (RFI) flagging in response to new geostationary sources.

For more details, see the Remote Sensing Systems RFI page:

- Replacement of the Geostationary_Satellite_Glint_Angle field with two new fields:
    - Geostationary_Reflection_Latitude
    - Geostationary_Reflection_Longitude
- For each observation, L2A now includes the location where the reflection vector intersects the geostationary sphere

5 RELATED DATA SETS

- AMSR-E/Aqua Daily EASE-Grid Brightness Temperatures
- AMSR-E/Aqua Daily Global Quarter-Degree Gridded Brightness Temperatures
- DMSP SSM/I-SSMIS Daily Polar Gridded Brightness Temperatures
- DMSP SSM/I-SSMIS Pathfinder Daily EASE-Grid Brightness Temperatures
- Near-Real-Time DMSP SSM/I-SSMIS Daily Polar Gridded Brightness Temperatures
- NIMBUS-5 ESMR Polar Gridded Brightness Temperatures
- NIMBUS-7 SMMR Antenna Temperatures
- NIMBUS-7 SMMR Pathfinder Brightness Temperatures
- Nimbus-7 SMMR Pathfinder Daily EASE-Grid Brightness Temperatures
- Nimbus-7 SMMR Polar Gridded Radiances and Sea Ice Concentrations

6 CONTACTS AND ACKNOWLEDGMENTS

Dr. Peter Ashcroft and Dr. Frank Wentz
Remote Sensing Systems
Santa Rosa, CA

7 REFERENCES

Ashcroft, Peter and Frank Wentz. 2000. Algorithm Theoretical Basis Document: AMSR Level-2A Algorithm, Revised 03 November. Santa Rosa, California USA: Remote Sensing Systems. (PDF file, 610 KB)

Conway, D. 2002. Advanced Microwave Scanning Radiometer - EOS Quality Assurance Plan. Huntsville, AL: Global Hydrology and Climate Center.

Japan Aerospace Exploration Agency (JAXA). Aqua AMSR-E Level 1 Product Format Description Document

Marquis, M., Richard Armstrong, Peter Ashcroft, Mary Jo Brodzik, D. Conway, Siri Jodha Singh Khalsa, E. Lobl, J. Maslanik, Julienne. Stroeve, and Vince Troisi. 2002.Research Applications and Opportunities Using Advanced Microwave Scanning Radiometer-Earth Observing System (AMSR-E) Data (poster). International Society for Optical Engineering Symposium (SPIE), Hangzhou, China, October 23-27, 2002.

For more information regarding related publications, see AMSR-E.

8 DOCUMENT INFORMATION

8.1 Publication Date

March 2003

8.2 Date Last Updated

30 March 2021

APPENDIX A – LEVEL-2A DATA FIELDS

Refer to Table A - 1. Notations Used in Document for the notations used throughout this document.

Table A - 1. Notations Used in Document

Notation	Description
Int8	8-bit (1-byte) signed integer
Int16	16-bit (2-byte) signed integer
Int32	32-bit (4-byte) signed integer
Uint8	8-bit (1-byte) unsigned integer
Uint16	16-bit (2-byte) unsigned integer
Float32	32-bit (4-byte) floating-point integer
Float64	64-bit (8-byte) floating-point integer
Char	8-bit character
Res. 1	56-km footprint
Res. 2	37-km footprint
Res. 3	21-km footprint
Res. 4	11-km footprint
Res. 5	5-km footprint
JAXA	Japan Aerospace Exploration Agency
RSS	Remote Sensing Systems (U.S.)

Note: For data with scale and offset values, the data values can be obtained in the specified units with the following equation:

Data value in units = (stored data value * scale factor) + offset

Example: T_b ;(kelvin) = (stored data value * 0.01) + 327.68

Scaling factors and offsets are provided with the local attributes of each HDF-EOS file. You should check each file to ensure correct values.

For more information on the L1 data fields' format descriptions transferred to L2A, see AMSR-E.

Low_Res_Swath Data Fields

Table A - 2. Low_Res_Swath_Data_Fields

Field	Type	Dimensions per Scant	Units	Scale Factor	Offsets	Source
Antenna_Temp_Coefficients_6_to_52	12 x 3	kelvin, kelvin/count, kelvin/countsq	n/a	n/a	RSS	JAXA
Data_Quality	Float32	128	n/a	n/a	n/a	JAXA
Observation_Supplement	Uint16	27	n/a	n/a	n/a	JAXA
Interpolation_Flag_6_to_52	Int8	12 x 16	n/a	n/a	n/a	JAXA
Position_in_Orbit	Float64	1	JAXA_convention_for_fractional_orbit	n/a	n/a	JAXA
Navigation_Data	Float32	6	m, m/s	n/a	n/a	JAXA
Attitude Data	Float32	3	degree	n/a	n/a	JAXA
SPC_Temperature_Count	Uint16	20	count	n/a	n/a	JAXA
Earth_Incidence	Int16	243	degree	0.0050	n/a	JAXA
Earth_Azimuth	Int16	243	degree	0.01	n/a	JAXA
Sun_Elevation	Int16	243	degree	0.1	n/a	JAXA
Sun_Azimuth	Int16	243	degree	0.1	n/a	JAXA
RX_Offset_Gain_Count	Uint16	32	count	n/a	n/a	JAXA
SPS_Temperature_Count	Uint16	32	count	n/a	n/a	JAXA
Land/Ocean_Flag_for_6_10_18_23_36_50_89A	Uint8	243 x 7	%	n/a	n/a	JAXA
Cold_Sky_Mirror_Count_6_to_52	Int16	16 x 12	radiometer_counts	n/a	n/a	JAXA

Field	Type	Dimensions per Scant	Units	Scale Factor	Offsets	Source
Hot_Load_Count_6_to_52	Int16	16 x 12	radiometer_counts	n/a	n/a	JAXA
6.9V_Res.1_TB_(not-resampled) 6.9H_Res.1_TB_(not-resampled) 10.7V_Res.2_TB_(not-resampled) 10.7H_Res.2_TB_(not-resampled) 18.7V_Res.3_TB_(not-resampled) 18.7H_Res.3_TB_(not-resampled) 23.8V_Approx._Res.3_TB_(not-resampled) 23.8H_Approx._Res.3_TB_(not-resampled) 36.5V_Res.4_TB_(not-resampled) 36.5H_Res.4_TB_(not-resampled)	Int16	243	kelvin	0.01	327.68	RSS, calculated from JAXA counts

6.9V_Res.1_TB 6.9H_Res.1_TB 10.7V_Res.1_TB 10.7V_Res.2_TB 10.7H_Res.1_TB 10.7H_Res.2_TB 18.7V_Res.1_TB 18.7V_Res.2_TB 18.7H_Res.1_TB 18.7H_Res.2_TB 23.8V_Res.1_TB 23.8V_Res.2_TB 23.8V_Res.3_TB 23.8H_Res.1_TB 23.8H_Res.2_TB 23.8H_Res.3_TB 36.5V_Res.1_TB 36.5V_Res.2_TB 36.5V_Res.3_TB 36.5H_Res.1_TB 36.5H_Res.2_TB 36.5H_Res.3_TB 89.0V_Res.1_TB 89.0V_Res.2_TB 89.0V_Res.3_TB 89.0V_Res.4_TB 89.0H_Res.1_TB 89.0H_Res.2_TB 89.0H_Res.3_TB 89.0H_Res.4_TB	Int16	243	kelvin	0.01	327.68	RSS
Scan_Quality_Flag	Int32	1	flag	n/a	n/a	RSS

Field	Type	Dimensions per Scant	Units	Scale Factor	Offsets	Source
Channel_Quality_Flag_6_to_52	Int16	12	flag	n/a	n/a	RSS
Resampled_Channel_Quality_Flag	Int16	30	flag	n/a	n/a	RSS
Effective_Cold_Space_Temperature_6_to_52	Float32	12	kelvin	n/a	n/a	RSS
Effective_Hot_Load_Temperature_6_to_52	Float32	12	kelvin	n/a	n/a	RSS
Res1_Surf Res2_Surf Res3_Surf Res4_Surf	Int8	243	%land	0.4	n/a	RSS
Sun_Glint_Angle	Int16	243	degree	0.01	n/a	RSS
Geostationary_Reflection_Latitude	Int16	243	degree	0.01	n/a	RSS
Geostationary_Reflection_Longitude	Int16	243	degree	0.01	n/a	RSS

High_Res_A_Swath and High_Res_B_Swath Data Fields

See Notations Used in this Document for notation definitions.

Beginning 4 November 2004, the 89 GHz A-horn developed a permanent problem resulting in a loss of those observations. Consequently, after 3 November 2004, the High_Res_A_Swath data fields contain values of 0.

Table A - 3. High_Res_A_Swath and High_Res_B_Swath Data Fields

Element	Type	Dimension per Scan	Unit	Scale Factor	Offset	Source
Antenna_Temp_Coefficients_89A	Float32	2 x 3	kelvin, kelvin/count, kelvin/countsq	n/a	n/a	RSS

Element	Type	Dimension per Scan	Unit	Scale Factor	Offset	Source
Interpolation_Flag_89_A	Int8	2 x 32	n/a	n/a	n/a	RSS
Cold_Sky_Mirror_Count_89A	Int16	32 x 2	radiometer_counts	n/a	n/a	JAXA
Hot_Load_Count_89A	Int16	32 x 2	radiometer_counts	n/a	n/a	JAXA
89.0V_Res.5A_TB_(not-resampled)	Int16	486	kelvin	0.01	327.68	RSS
89.0H_Res.5A_TB_(not-resampled)	Int16	486	kelivn	0.01	327.68	RSS
Scan_Quality_Flag_89A	Int32	1	flag	n/a	n/a	RSS
Channel_Quality_Flag_89A	Int16	2	flag	n/a	n/a	RSS
Effective_Cold_Space_Temperature_89A	Float32	2	kelvin	n/a	n/a	RSS
Effective_Hot_Load_Temperature_89A	Float32	2	kelvin	n/a	n/a	RSS
Res5A_Surf	Int8	486	%land	4.0	n/a	RSS

Geolocation Fields

See Notations used in this document for notation definitions.

The Geolocation fields for the High_Res_A_Swath and the High_Res_B_Swath are completely analogous to those of the Low_Res_Swath with 486 observations per scan rather than 243.

Table A - 4. Geolocation Fields

Field	Type	Dimension per scan	Source	Units
Time	Float64	1	JAXA	TAI93 (seconds since midnight, 01 January 1993)
Latitude	Float32	243	RSS	degree
Longitude	Float32	243	RSS	degree

Global Attributes

See Notations used in this document for notation definitions.

The swath attribute fields of the High_Res_A_Swath and the High_Res_B_Swath are identical to those of the Low_Res_Swath except that the Resampled_Channel_Sequence field is omitted because high-resolution swaths have no resampled channels. Also, the Level1A_Channel_Sequence field was modified to describe the order of the elements of the High_Res_A_Swath Level1A_Scan_Chan_Quality_Flag rather than that of the Low_Res_Swath quality flag

Table A - 5. Global Attributes

Attribute	Type	Description
HDFEOSVersion	Char	HDF-EOS Version of product
StructMetadata.0	Char	HDF-EOS structural metadata
ProcessingLevelID	Char	Product processing level
ProcessingFacility	Char	Product processing facility
SensorShortName	Char	Sensor short name
EquatorCrossingLongitude	Char	Longitude at which instrument crosed equator
OrbitSemiMajorAxis	Char	Diameter of platform orbit at the equator
OrbitEccentricity	Char	How far the elliptical platform orbit deviates from a circle
OrbitArgumentPerigee	Char	Point at which platform orbit is closest to Earth in degrees from ascending equatorial node

Attribute	Type	Description
OrbitInclination	Char	Degree by which platform orbit deviates from polar (north / south) orbit
OrbitPeriod	Char	Orbit period in minutes
EllipsoidName	Char	Reference ellipsoid name
SemiMajorAxisofEarth	Char	Diameter of Earth (geoid) at the equator
FlatteningRatioofEarth	Char	The amount by which the polar geoid diameter is smaller than the equatorial geoid diameter
L1AProductionDataTime	Char	Production date and time of input L1A file
L1ANumerofMissingScans	Char	Number of missing scans in input L1A file
L2AProcessingDate	Char	Production date and time of L2A file
PlatformShortName	Char	Platform short name
EquatorCrossingTime	Char	Time at which instrument crossed equator
EquatorCrossingDate	Char	Date at which instrument crossed equator
EphemerisType	Char	Definitive or Predicted
EphemerisGranulePointer	Char	Ephemeris input file
EphemerisQA	Char	Ephemeris Quality Assessment
NumberofMissingPackets	Char	Number of missing L1A packets, generally from spacecraft to ground transmission
QAPercentParityErrorData	Char	Percent parity error on spacecraft to ground transmission
Altitude	Char	Average altitude of instrument above geoid
RangeBeginningDate	Char	Beginning date of file coverage
RangeBeginningTime	Char	Beginning time of file coverage
RangeEndingDate	Char	Ending date of file coverage
RangeEndingTime	Char	Ending time of file coverage
InputPointer	Char	Input L1A file
PlatinumThermistorWbCoeff	Char	Thermistor Count to Temperature Coefficients: T = Wc + Wb (counts - segment)
PlatinumThermistorWcCoeff	Char	Thermistor Count to Temperature Coefficients: T = Wc + Wb (counts - segment)
PlatinumThermistorSegment	Char	Thermistor Count to Temperature Coefficients: T = Wc + Wb (counts - segment)
CoefficientAvv	Char	APC Coefficients: Tbv = Avv * Tav + Ahv * Tah + Aov
CoefficientAhv	Char	APC Coefficients: Tbv = Avv * Tav + Ahv * Tah + Aov
CoefficientAovTimesCold	Char	APC Coefficients: Tbv = Avv * Tav + Ahv * Tah + Aov
CoefficientAhh	Char	APC Coefficients: Tbh = Ahh * Tah + Avh * Tav + Aoh
CoefficientAvh	Char	APC Coefficients: Tbh = Ahh * Tah + Avh * Tav + Aoh

Attribute	Type	Description
CoefficientAohTimesCold	Char	APC Coefficients: Tbh = Ahh * Tah + Avh * Tav + Aoh
PGE_Version	Char	Product maturity code and version number
StartOrbitNumber	Float32	Orbit number at start of data acquisition
StopOrbitNumber	Float32	Orbit number at stop of data acquisition
OrbitDirection	Char	Direction of orbit (ascending or descending)
NumberofScans	Int32	Number of scans
SoftwareRevisionDate	Char	Date of last product software revision
CoreMetadata.0	Char	HDF-EOS core metadata